31. Line, J. M., ter Braak, C. J. F. & Birks, H. J. B. WACALIB version 3. 3: A computer program to reconstruct environmental variables from fossil assemblages by weighted averaging and to derive sample-specific errors of prediction. *J. Paleolimnol.* **10,** 147–152 (1994).

Supplementary information is available on *Nature*'s World-Wide web site (http://www.nature. com) or as paper copy from the London editorial office of *Nature*.

Acknowledgements

We thank K. Mavuti, B. Ammann, F. Janssen and H. E. Wright for field assistance; the Lake Naivasha Riparian Association for lake access; F. Gasse for use of the African diatom reference and calibration data sets; and S. Fritz, F. Gasse, K. Kelts, F. Oldfield, J. P. Smol, B. Tinsley and H. E. Wright for comments on the manuscript. This work was supported by NSF, the Quaternary Paleoecology Program at the University of Minnesota, and by fellowships from NOAA and FWO-Vlaanderen (D.V.) The fieldwork was conducted with permission from the Office of the President of the Republic of Kenya to K. Mavuti.

Correspondence should be addressed to D.V. (e-mail: dirk.verschuren@rug.ac.be). The data presented here are archived at the World Data Center-A for Paleoclimatology.

Precise climate monitoring using complementary satellite data sets

Frank J. Wentz & Matthias Schabel

Remote Sensing Systems, 438 First Street, Suite 200, Santa Rosa, California 95401, USA

Observations from Earth-orbiting satellites have been a key component in monitoring climate change for the past two decades. This has become possible with the availability of air temperatures from the Microwave Sounding Unit (MSU)[1] since 1979, sea surface temperatures from the Advanced Very High Resolution Radiometer (AVHRR)[2] since 1982 and, most recently, measurements of atmospheric water vapour content from the Special Sensor Microwave Imager (SSM/I)[3] since 1987. Here we present a detailed comparison of each pair of these three time series, focusing on both interannual and decadal variations in climate. We find a strong association between sea surface temperature, lower-tropospheric air temperature and total column water-vapour content over large oceanic regions on both time scales. This lends observational support to the idea of a constant relative humidity model having a moist adiabatic lapse rate. On the decadal timescale, the combination of data sets shows a consistent warming and moistening trend of the marine atmosphere for 1987–1998.

The detection and measurement of small changes in the Earth's climate require extremely precise global observations of a broad spectrum of complementary physical variables. In this endeavour, satellite observations are playing an increasingly important role. As compared to conventional *in situ* observations, satellites provide daily near-global coverage with a very high statistical precision that results from averaging millions of individual observations. Here we present a three-way intercomparison of three satellite-derived climate variables that are closely correlated in the marine boundary layer and lower troposphere: sea surface temperature T_S, lower-tropospheric air temperature T_A, and vertically integrated, or columnar, atmospheric water vapour W. This intercomparison allows us to determine the coupling of the three variables on interannual and decadal timescales and investigate the accuracy of the individual time series[4,5,6].

The T_A and T_S data sets are standard products that have been available for some time[1,2], whereas the W data set is a relatively new product[3] beginning in 1987 with the launch of the special sensor microwave imager (SSM/I), a multichannel microwave radiometer. Since 1987 four more SSM/Is have been launched, providing an uninterrupted 12-year time series. Imaging radiometers before SSM/I were poorly calibrated, and as a result early water-vapour studies[7] were unable to address climate variability on interannual and decadal timescales.

To retrieve water vapour from the SSM/I observations, we use a physically based algorithm that simultaneously computes water vapour, wind speed, and cloud water by directly matching the observations to a radiative transfer model[3]. The primary channel for W is at 22 GHz, which is centred on a water-vapour absorption line. Additional dual-polarization channels at 19 and 37 GHz are used to remove crosstalk (that is, a signal from one variable aliasing into another) attributable to wind and clouds. A monthly climatology is used to specify the regional and seasonal variations of T_S. The T_A and T_S decadal time series are used to remove a small crosstalk component on interannual timescales. This correction for interannual crosstalk is quite small, reducing the amplitude of the interannual variability in W by about 8%. Other water-vapour retrieval algorithms have been developed, but most do not fully account for crosstalk or do not use the 22-GHz channel[8,9], thereby limiting their ability to measure the small interannual climate signal. The retrieval of W requires the radiometrically cold background of the sea surface and cannot be done over land, which is highly emissive.

For the intercomparisons, we use Reynolds' 1982–1998 optimally interpolated sea surface temperature data set[2] and the 1979–1998 version-c1 MSU lower-tropospheric air temperature[10] with a correction for orbital decay that is added to the zonal averages[6]. (We do not use the new version-d MSU product because it has not yet been published. However, for the intercomparison period (1987–1998) over the oceans, there is little difference (0.01 K per decade) between version c1 plus orbit decay and version d.) The three variables are geographically and temporally sampled in the same manner to ensure an unbiased comparison. Figure 1 shows the deseasonalized anomalies of W, T_S, and T_A. Results are shown for three zones: the northern extratropics (20 °N–60 °N), the tropics (20 °N–20 °S), and the southern extratropics (20 °S–60 °S). The seasonal cycle has been removed and the residuals have been low-pass filtered by convolution with a gaussian distribution having a ±90-day width at half-peak value. The variation of water vapour with latitude is large (5–60 mm), so it is more convenient to express W in terms of a percentage change. To compute percentages, the daily zonal W is divided by the 12-year mean value for the zone. The prominent El Niño/Southern Oscillation signal is clearly evident in the tropics, peaking in January 1983, December 1987 and December 1997. For the 1983 and 1997 El Niños, the T_S signal leads T_A by a few months, but the 1987 El Niño shows no such lag. The scaling in Fig. 1 is based on radiosonde observations of mid-latitude seasonal variability, which show $\Delta W/\Delta T_S = 11\%\ K^{-1}$ and $\Delta T_A/\Delta T_S = 1.6$. To display this scaling, the T_A time series have been divided by 1.6, and the vapour scale on the right side of the figure is chosen so that 11% = 1 K.

Three statistics for the 1987–1998 period are given in Table 1: the correlation coefficient, the decadal trend, and the scaling coefficient, which is the ratio of standard deviations of the time series. The three variables are closely coupled, as has been shown by previous studies on shorter timescales of 2–5 years (refs 9 and 11). In the tropics, where the El Niño/Southern Oscillation cycle dominates the interannual variability, the correlation coefficients are very high: W with T_S is 0.98, W with T_A is 0.93, and T_S with T_A is 0.94. The corresponding tropical scaling coefficients are $\Delta W/\Delta T_S = 9.2\%\ K^{-1}$, $\Delta T_A/\Delta T_S = 1.4$ and $\Delta W/\Delta T_A = 6.7\%\ K^{-1}$, which are similar to the mid-latitude radiosonde seasonal scalings. These tropical scaling relationships are consistent with a constant relative humidity (H_{rel}) model having a moist adiabatic lapse rate (MALR)[12]. The Clausius–Clapeyron equation for saturation vapour pressure[13] predicts that the water-vapour density, and hence columnar content, increases

with air temperature if H_{rel} stays constant. The rate of increase varies from 6.0% to 7.5%, depending on air temperature, with a value near 6.7% K^{-1} for the tropics. Other satellite studies[7,8,11] on the seasonal variability of W, when averaged zonally, also support the constant-H_{rel} assumption.

According to the MALR model, T_A variability is greater than T_S variability, as is shown by the satellite observations. For example, if T_S is 293K (294K), MALR gives a temperature of 276.4 K (277.8) at 3.5 km. Thus a change of 1K at the surface corresponds to a change of 1.4 K at an altitude of 3.5 km, which is the nominal altitude for the MSU T_A. We are assuming the surface air temperature equals T_S, which is generally the case over the ocean to within a few tenths of a degree. Although significant differences have been observed between the MALR and the actual lapse rate for some environments such as over cold land surfaces[12], the MALR is in good agreement with *in situ* observations over the ocean. We compared the MALR averaged over the lower 3.5 km of the troposphere with radiosonde observations from 56 small islands around the world during 1987–1991 and found a mean and r.m.s. difference of –0.2 K km^{-1} and 1.0 K km^{-1}, respectively.

Our results for large-scale zonal averages differ from radiosonde regional studies[14], which show a relatively weak W versus T_A correlation on interannual timescales. The weak correlation is probably due to regional variability in atmospheric stratification and convection. It appears that the zonal averaging effectively cancels the regional variability and produces a result that is well represented by the relatively simple constant-H_{rel} MALR model. However, this model is only applicable for large zonal averages, and not necessarily to regional processes.

We now examine the decadal trends for the 1987–1998 period. Long-term trends are a difficult statistic to derive from satellite data because of problems with satellite intercalibration and sensor drift[4,5,6,10]. However, such trends are important because they may be indicators of anthropogenic climate change. Although a 12-year period is relatively short for inferring decadal trends, the time period does give us the opportunity to compare three independent data sets. As the measurement errors in the three records are largely independent, the three time series, in combination, may be capable of defining the climate trends with greater confidence than any one of them by itself.

In the tropics the trends are 2.1% per decade, 0.23 K per decade, and 0.22 K per decade for W, T_S and T_A , whereas the global trends are 1.8% per decade, 0.15 K per decade, and 0.10 K per decade, respectively. The ratio of the W and T_S trends closely matches the seasonal and interannual scaling coefficient. However, the ratio of the T_A and T_S trends ranges between 0.7 and 1, rather than the 1.4 scaling exhibited by the interannual variability. It is not clear if this discrepancy is real or due to small sensor-calibration problems. The overlap interval between the T_S and T_A time series extends back to 1982, which allows for the comparison of these two variables on a longer timescale. The tropical and global 1982–1998 decadal trends for T_S are 0.13 K per decade and 0.12 K per decade and for T_A are 0.20 K per decade and 0.19 K per decade respectively, revealing a T_A/T_S scaling consistent with the seasonal and interannual scaling. On the longest timescale of 1979–1998, for which only the MSU data are available, the tropical and global T_A trends are 0.12 K per decade and 0.13 K per decade, respectively.

Regional radiosonde studies have also indicated a warming and moistening of the atmosphere over the last 10–20 years. Vapour trends over North America from 1973–1993 were reported to be 3–7% per decade[15] and to be 1% per decade over China from 1970–1990 (ref. 16). *In situ* observations also show a general warming and moistening over the tropical Pacific from the early 1970s to the early 1990s (refs 14 and 17). An apparent contradiction to these results is a study involving satellite vapour retrievals from infrared observations that reports widespread drying in the tropics from 1979–1995 (ref. 18). However, inferring vapour trends from infrared measurements is difficult, requiring continuous calibration to radiosondes, and it appears that the reported drying is probably spurious, caused by problems with the radiosondes used for calibration[19].

The decadal trend for W comes from a least-squares fit to deseasonalized zonal daily averages. There are two ways to interpret the statistical significance of this decadal trend. First, if interannual variability is considered to be a source of noise masking the linear trend, then the time series can be modelled as a first-order autoregression[20]. By computing the lag-1 correlation coefficient and the residual variance, we find that the standard error in the trend estimate is 0.5% per decade for the tropics and 0.3% per decade globally. Second, the trend may be interpreted as a first-order statistic of the interannual variability, with the only source of error being the satellites' ability to measure the true daily zonal averaged W. This satellite measurement error, which results from retrieval error and incomplete spatial/temporal sampling, is estimated by comparing simultaneous observations from different satellites. We find that the standard error in the daily W is 1.5%

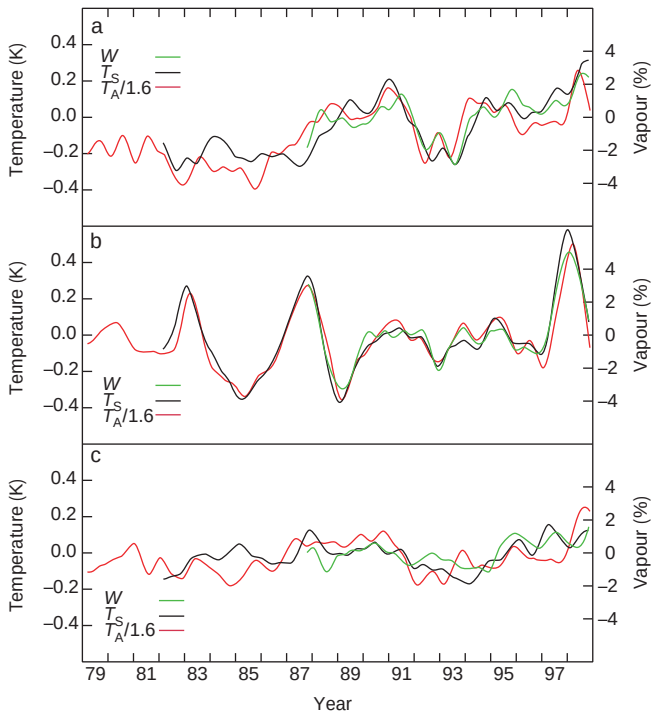

Figure 1 Anomaly time series of three climate variables. **a, b, c,** Water vapour W (green), sea surface temperature T_S (black), and air temperature T_A (red) are shown for the northern extratropics (20 °N–60 °N; **a**), tropics (20 °S–20 °N; **b**), and southern extratropics (20 °S–60 °S; **c**). Air temperature is divided by 1.6.

Table 1 Statistics on interannual and decadal variability

	20 °N–60 °N	20 °S–20 °N	20 °S–60 °S
Decadal trend			
W (% per decade)	1.9	2.1	1.0
T_s (K per decade)	0.20	0.23	0.03
T_A (K per decade)	0.04	0.22	0.00
Correlation			
W with T_s	0.84	0.98	0.73
W with T_A	0.71	0.93	0.36
T_A with T_S	0.69	0.94	0.56
Scaling coefficient			
W/T_S (% K^{-1})	8.5	9.2	8.6
W/T_A (% K^{-1})	6.8	6.7	4.6
T_A/T_S	1.2	1.4	1.9

and is uncorrelated from one day to the next. This gives a standard error in the trend estimate of 0.08% per decade[20]. An additional error is the uncertainty in determining the intersatellite biases, which are estimated from data collected during periods of satellite overlap (1–4 years). Monte Carlo simulations show that the uncertainty in specifying the intersatellite biases introduces a 0.2% per decade standard error in the trend estimate. These estimates of trend error do not include the additional uncertainty involved with questions of prediction or representation (that is, how well the 1987–1998 period represents longer-term climate change).

As a check on the error analysis, we divide the SSM/I data into two sets: local morning and local evening. For each set, completely independent derivations of the decadal trends for the three latitude zones give a maximum difference between the morning and evening trends of 0.2% per decade. This agreement indicates that diurnal effects only weakly influence the SSM/I data, in marked contrast to the significant diurnal problems affecting the MSUs. A complicated procedure is required to remove the diurnal effect from the MSU observations[10], and this possibly introduces spurious trends.

The retrieval of W from SSM/I observations is less problematic than the T_S and T_A retrievals in other ways as well. The 22-GHz radiance observed by SSM/I is directly related to W, whereas the MSU measures the middle-to-upper troposphere and then infers the lower-tropospheric temperature[21]. Furthermore, assuming a constant H_{rel}, the 22-GHz water-vapour radiance is three times more sensitive to changes in air temperature than MSU 54-GHz radiance. For AVHRR, a continuous calibration with *in situ* data is required to remove the cooling effect of atmospheric aerosols such as those emitted by volcanic eruptions[22] and to correct for instrument drift and intersatellite biases[2]. The robustness and accuracy of the SSM/I W retrieval makes it a useful validation tool for the more complex retrievals of T_A and T_S, although we must keep in mind that they are different physical variables.

The consistency we now see emerging from various satellite observations provides new information on climate dynamics and should help resolve some of the past controversies concerning errors in the satellite data. It is notable that a relatively simple constant-H_{rel} plus MALR model closely predicts the observed interannual and decadal variations of W, T_S and T_A when zonally averaged over the tropics. Furthermore, the evidence here shows that the marine atmosphere has significantly warmed and moistened over the past decade.

Received 8 March; accepted 26 November 1999.

1. Spencer, R. W. & Christy, J. R. Precise monitoring of global temperature trends from satellites. *Science* **247,** 1558–1562 (1990).
2. Reynolds, R. W. & Smith, T. M. Improved global sea surface temperature analyses using optimum interpolation. *J. Clim.* **7,** 929–948 (1994).
3. Wentz, F. J. A well-calibrated ocean algorithm for special sensor microwave/imager. *J. Geophys. Res.* **102,** 8703–8718 (1997).
4. Hurrell, J. W. & Trenberth, K. E. Spurious trends in satellite MSU temperatures from merging different satellite records. *Nature* **386,** 164–167 (1997).
5. Hurrell, J. W. & Trenberth, K. E. Difficulties in obtaining reliable temperature trends: reconciling the surface and satellite microwave sounding unit records. *J. Clim.* **11,** 945–967 (1998).
6. Wentz, F. J. & Schabel, M. Effects of satellite orbital decay on MSU lower tropospheric temperature trends. *Nature* **394,** 661–664 (1998).
7. Stephens, G. L. On the relationship between water vapor over the oceans and sea surface temperature. *J. Clim.* **3,** 634–645 (1990).
8. Jackson, D. L. & Stephens, G. L. A study of SSM/I-derived columnar water vapor over the global oceans. *J. Clim.* **8,** 2025–2038 (1995).
9. Randel, D. L. *et al.* A new global water vapor dataset. *Bull. Am. Meteorol. Soc.* **77,** 1233–1246 (1996).
10. Christy, J. R., Spencer, R. W. & Lobl, E. S. Analysis of the merging procedure for the MSU daily temperature time series. *J. Clim.* **11,** 2016–2041 (1998).
11. Bony, S., Duvel, J. -P. & Le Treut, H. Observed dependence of the water vapor and clear-sky greenhouse effect on sea surface temperature: comparison with climate warming experiments. *Clim. Dyn.* **11,** 307–320 (1995).
12. Stone, S. H. & Carlson, J. H. Atmospheric lapse rate regimes and their parameterization. *J. Atmos. Sci.* **36,** 415–423 (1979).
13. Peixoto, J. P. & Oort, A. H. *Physics of Climate* (American Institute of Physics Press, New York, 1991).
14. Gaffen, D. J., Elliott, W. P. & Robock, A. Relationships between tropospheric water vapor and surface temperature as observed by radiosondes. *Geophys. Res. Lett.* **19/18,** 1839–1842 (1992).
15. Ross, R. J. & Elliott, W. P. Tropospheric water vapor climatology and trends over north America: 1973–93. *J. Clim.* **9–12,** 3561–3574 (1996).
16. Zhai, P. & Eskridge, R. E. Atmospheric water vapor over China. *J. Clim.* **10,** 2643–2652 (1997).
17. Gutzler, D. Low-frequency ocean–atmosphere variability across the tropical western Pacific. *J. Atmos. Sci.* **53,** 2773–2785 (1996).
18. Schroeder, S. R. & McGuirk, J. P. Widespread tropical atmospheric drying from 1979 to 1995. *Geophys. Res. Lett.* **25–9,** 1301–1304 (1998).
19. Ross, R. J. & Gaffen, D. J. Comment on Widespread tropical atmospheric drying from 1979 to 1995, by Schroeder and McGuirk. *Geophys. Res. Lett.* **25–23,** 4357–4358 (1998).
20. Wilks, D. S. *Statistical Methods in the Atmospheric Sciences* (Academic, New York, 1995).
21. Spencer, R. W. & Christy, J. R. Precision and radiosonde validation of satellite gridpoint temperature anomalies. Part II: A tropospheric retrieval and trends during 1979–1990. *J. Clim.* **53,** 858–866 (1992).
22. Reynolds, R. W. Impact of Mount Pinatubo aerosols on satellite-derived sea surface temperatures. *J. Clim.* **6,** 768–775 (1993).

Acknowledgements

This work was supported by NASA as part of their pathfinder Data Set program.

Correspondence and requests for materials should be addressed to F.J.W. (e-mail: wentz@remss.com).

The Pleistocene serpent *Wonambi* and the early evolution of snakes

John D. Scanlon*† & Michael S. Y. Lee*

* *Department of Zoology, University of Queensland, Brisbane QLD 4072, Australia*

† *Department of Biological Sciences, University of New South Wales, Sydney, NSW 2052, Australia*

The Madtsoiidae were medium sized to gigantic snakes with a fossil record extending from the mid-Cretaceous to the Pleistocene, and spanning Europe, Africa, Madagascar, South America and Australia[1–3]. This widely distributed group survived for about 90 million years (70% of known ophidian history), and potentially provides important insights into the origin and early evolution of snakes. However, madtsoiids are known mostly from their vertebrae, and their skull morphology and phylogenetic affinities have been enigmatic. Here we report new Australian material of *Wonambi*, one of the last-surviving madtsoiids[4–6], that allows the first detailed assessment of madtsoiid cranial anatomy and relationships. Despite its recent age, which could have overlapped with human history in Australia, *Wonambi* is one of the most primitive snakes known—as basal as the Cretaceous forms *Pachyrhachis*[7] and *Dinilysia*[8]. None of these three primitive snake lineages shows features associated with burrowing, nor do any of the nearest lizard relatives of snakes (varanoids). These phylogenetic conclusions contradict the widely held 'subterranean' theory of snake origins[9–12], and instead imply that burrowing snakes (scolecophidians and anilioids) acquired their fossorial adaptations after the evolution of the snake body form and jaw apparatus in a large aquatic or (surface-active) terrestrial ancestor.

Serpentes Linnaeus, 1758
Madtsoiidae Hoffstetter, 1961
Wonambi Smith, 1976

Revised diagnosis. Neural spines of vertebrae high, sloping, posterodorsally, with sharp-edged anterior lamina extending to near anterior edge of zygosphene; transverse processes extending laterally beyond zygaphophyses in most trunk vertebrae, synapophyses with concave dorsal edge in lateral view; zygosphene relatively narrow, with steep facets (20–30° from vertical); zygapophyses inclined 20° or more above horizontal; haemal keel in middle and posterior trunk region narrow and weakly defined laterally, but often distinctly bifid or trifid on the posterior third of the centrum.